Int. J. Anal. Appl. (2025), 23:35

International Journal of Analysis and Applications

Decision-Making Regarding a Novel Bounded Exponentiated Weibull Mixture Model Is Applied to Certain Observed Data

Arafa O. Mustafa[1], Nhla A. Abdalrahman[2], Malak S. S. Hussain[3], Nazzik I. M. Mohammed[4,9], Salah H. Alshabhi[5], Mustafa M. Mohammed[5], Mona Magzoub[6], Nidal E. Taha[7], Awad A. Bakery[5,8,*]

[1]*University of Jeddah, College of Business at Khulis, Jeddah, Saudi Arabia*
[2]*Department of Human Resource Management, College of Business, University of Jeddah, Jeddah, Saudi Arabia*
[3]*University of Jeddah, College of Business at Alkamil, Department of Human Resources Management, Jeddah, Saudi Arabia*
[4]*Foreign Languages Department, Faculty of Arts and Humanities -Al Baha University, Saudi Arabia*
[5]*University of Jeddah, Applied college at Khulis, Department of Mathematics, Jeddah, Saudi Arabia*
[6]*Mathematics Department, Applied college at Alkamil, University of Jeddah, Saudi Arabia*
[7]*Department of Mathematics, College of Science, Qassim University, Buraidah 51452, Saudi Arabia*
[8]*Department of Mathematics, Faculty of Science, Ain Shams University, Cairo, Egypt*
[9]*English Language Department, Faculty of Education, University of Gezira, Hasahesia, Sudan*

[*]*Corresponding author:* awad_bakery@yahoo.com

Abstract. The exponentiated Weibull mixture model (EWMM) is the most frequently used probability distribution in the disciplines of reliability engineering and applied linguistics. Exponentiated Weibull distributions, on the other hand, are unbounded. A variety of applications digitalize the monitored data and have bounded service regions. Different types of double truncated Weibull mixture models (BEWMM) are discussed in this article. These include the double truncated exponential mixture model (BEMM), the double truncated Rayleigh mixture model (BRMM), the double truncated Weibull mixture model (BWMM), and the double truncated generalized exponential mixture model (BGEMM). By combining a mixture model and bounded support regions, we can create a model that is extremely scalable and can capture a variety of statistical properties of the results, such as mean behavior, distribution, form, and tail behavior. We propose an alternative method for evaluating the model parameters, which aims to maximize the upper bound on the data log-likelihood function. We evaluate the (BEWMM) execution using simulated and actual data.

Received: Oct. 11, 2024.

2020 *Mathematics Subject Classification.* 62H12.

Key words and phrases. applied linguistics; decision-making; mixture model; bounded support regions; exponentiated Weibull distribution; goodness of-fit.

https://doi.org/10.28924/2291-8639-23-2025-35
ISSN: 2291-8639

1. Introduction and basic definitions

The finite mixture model provides a natural representation of heterogeneity in a finite number of latent classes. It concerns modelling a statistical distribution by a mixture (or weighted sum) of other distributions, such as, machine learning, design acknowledgment, and Bioinformatics. The basic purpose of enthusiasm of this methodology is in its capacity to utilize prior figuring out how to demonstrate the powerlessness probabilistically. Among the estimations in light of the Bayesian framework, the Weibull mixture model (WMM) ([1]- [3]) is a without a doubt comprehended technique used for by and large applications. An advantage of WMM is that it requires a little measure of parameters for learning. Also, these parameters can be profitably assessed by getting the expectation maximization (EM) figuring ([4]- [5]) to maximize the log-likelihood function. Notwithstanding the way that the WMM is a versatile and fit contraption for data examination, it is fragile to abnormalities and might provoke over the top influence capacity to little amounts of data core interests. Furthermore, for some associated issues, the tail of the Weibull distribution is taller than required. As of late, there has been a developing examination enthusiasm for a Bayesian system in light of the displaying of the probability density function of the information by means of the exponentiated Weibull distribution (EWD) ([6]- [8]). EWD has been effectively utilized as a part of image and video coding ([9] and [10]), composition segregation and recovery ([11]- [13]), change discovery [14], and image denoising [15]. This conveyance has one parameter (ν) more than the Weibull distribution. The parameter γ controls the tails of the distribution and makes sense of if the latter is beaten or level. It justifies indicating that the Weibull and Rayleigh distributions are particular cases for the exponentiated Weibull distribution, where $\nu = 1$; $\nu = 1$ and $\gamma = 2$, independently. Thusly, the exponentiated Weibull mixture model (EWMM) has the flexibility required to fit the condition of the data better than the Weibull mixture model (WMM). One drawback of the previously stated blend models is that their appropriations are unbounded with a supporting range of $(0, \infty)$. We extend all the past models to the double truncated case such that their disseminations are unbounded with a range $(-\infty, \infty)$. We find in various certified applications that the watched data constantly fall within the restricted reinforce territories ([16]- [18]). For instance, in the zone of sign handling, the force range is semi-limited. In the region of picture PC vision, the pixels are more often than not in the constrained extent. In ([19]- [22]), a double truncated Weibull mixture model (BWMM) was proposed for discourse preparing. Notwithstanding, in numerous applications, the tail of the Weibull distribution is taller than required. Likewise, the BWMM is not sufficiently adaptable to fit the state of the information. Roused by the previously stated perceptions, we present in this paper the high flexibility of a double truncated exponentiated Weibull mixture model (BEWMM) for examining information, which incorporates the EMM, WMM, RMM, GEMM, and BWMM, as special cases with less degree of freedom. Our methodology varies from those talked about above by the accompanying articulations. Firstly, there is a development of the exponentiated Weibull distribution in this paper. The BEWMM Model is of noticeable significance for image coding and

compression applications. This new distribution has a versatility to fit differing conditions of watched data, for instance, bounded support data and non-Gaussian. In addition, all aspects of our model can show the watched data with different restricted reinforce regions. Finally, to gage the parameters of the proposed model, we propose another technique, remembering the finished objective to open up the higher bound to the data log-likelihood function. We display through wide reenactments that the proposed model is superior to anything diverse methods considering the exhibit in the probability density function of the data by a method for constrained mix model. Whatever is left of this paper is created as takes after: Section 2 depicts the proposed method in purpose of interest; Section 3 demonstrates the parameter estimation; Section 4 sets out the trial results; and Section 5 shows our conclusions.

2. Proposed technique

Given a K parts of mixture model, the probability density function of the random variable x_i is

$$f(x_i|\Theta) = \sum_{j=1}^{K} \rho_j p(x_i|\theta_j), \tag{2.1}$$

where Θ addresses the model parameters. The prior probability ρ_j satisfies the prerequisites

$$\rho_j \geq 0 \text{ and } \sum_{j=1}^{K} \rho_j = 1. \tag{2.2}$$

As showed up in (2.1), the key goal of quantifiable showing is to develop a model that can best depict the measurable properties of the essential source. The mixture models have relied on upon to demonstrate the concealed distributions. Note that $p(x_i|\theta_j)$ can be any kind of distribution. In EMM ([23]- [24]), WMM ([25]- [27]), and EWMM ([7] and [8]), $p(x_i|\theta_j)$ is the exponential distribution $\phi(x_i|\mu_j, \beta_j)$, the Weibull distribution $\Upsilon(x_i|\mu_j, \beta_j, \gamma_j)$ and the exponentiated Weibull distribution $T(x_i|\mu_j, \beta_j, \nu_j, \gamma_j)$, individually. These distributions are all unbounded with support range $(0, \infty)$. We extend all the previous models to the double truncated case such that their distributions are unbounded with a support range $(-\infty, \infty)$. So along the paper we express the accompanying tradition that all the given models have two sided. Remembering the deciding objective to thrashing this issue, we propose another finite mixture model that has the flexibility to fit unmistakable conditions of watched data, for instance, non-Gaussian and bounded support data. To begin with, for each part (meant by Ω_j), we portray ∂_j to be the bounded support region in $\mathbb{R}$, and the marker function as

$$\delta(x_i|\Omega_j) = \begin{cases} 1, & \text{if } x_i \in \Omega_j \\ 0, & \text{if otherwise.} \end{cases} \tag{2.3}$$

With the marker function $\delta(x_i|\Omega_j)$ in (2.3), we characterize a double truncated exponentiated Weibull distribution

$$\mathrm{Y}_{ij} = \mathrm{Y}(x_i|\mu_j,\beta_j,\nu_j,\gamma_j) = \frac{T(x_i|\mu_j,\beta_j,\nu_j,\gamma_j)\delta(x_i|\Omega_j)}{\int_{\partial_j} T(x|\mu_j,\beta_j,\nu_j,\gamma_j)dx}, \tag{2.4}$$

The distribution in (2.4) is according to the accompanying:

$$T(x_i|\mu_j,\beta_j,\nu_j,\gamma_j) = \frac{\nu_j\gamma_j\beta_j}{2}|x_i-\mu_j|^{\gamma_j-1}\exp(-\beta_j|x_i-\mu_j|^{\gamma_j})(1-\exp(-\beta_j|x_i-\mu_j|^{\gamma_j}))^{\nu_j-1}, \tag{2.5}$$

where

$$\beta_j = \frac{1}{\sigma_j^{\gamma_j}}\Big[\nu_j\int_0^{\infty} x^{\frac{2}{\gamma_j}}e^{-x}(1-e^{-x})^{\nu_j-1}dx\Big]^{\frac{\gamma_j}{2}}. \tag{2.6}$$

The parameters μ_j, γ_j, ν_j, σ_j, and β_j are positive parameters corresponding to the mean, power, shape, standard deviation and scale, respectively. The BEWD is a very flexible family of distributions, it includes double truncated exponential, double truncated Generalized exponential, double truncated Rayleigh and double truncated Weibull as special cases. The parameter γ_j controls the tails of the distribution and figures out if the last is crested or level. In (2.4), $\int_{\partial_j} T(x|\mu_j,\beta_j,\nu_j,\gamma_j)dx$ is the standardization steady and is recognized as the offer of $T(x|\mu_j,\beta_j,\nu_j,\gamma_j)$ that has a place with the bounded support regions ∂_j. The thought to characterize the distribution Y_{ij} in (2.4) depends on the way that the watched information are digitalized and have bounded support. We relegate Y_{ij} as equivalent to $T(x|\mu_j,\beta_j,\nu_j,\gamma_j)$ in the support region ∂_j, and as zero outside. It justifies determining that the proposed appropriation in (2.4) will reliably satisfy the conditions of the probability density [28]:

$$\mathrm{Y} \geq 0 \text{ and } \int_{-\infty}^{\infty} \mathrm{Y}(x|\mu_j,\beta_j,\nu_j,\gamma_j)\,dx = 1. \tag{2.7}$$

Given the distribution $\mathrm{Y}(x_i|\mu_j,\beta_j,\nu_j,\gamma_j)$ in (2.4), the log-likelihood function is composed in the structure

$$L(\Theta) = \sum_{i=1}^{N}\log\sum_{j=1}^{K}\rho_j\mathrm{Y}_{ij}(x_i|\theta_j). \tag{2.8}$$

From (2.8), we can see that every segment of the proposed model can demonstrate the watched information with various bounded support regions ∂_j. We can characterize any shape taking into account the earlier information about the watched information. By looking at the scientific articulations of the proposed model with the EMM ([23], [24], [29] and [30]), we see that on the off chance that we set $\gamma_j = 1$, $\nu_j = 1$ and the bounded support region is relegated as $\delta(x_i|\Omega_j) = 1$ for every mark Ω_j, our strategy is like the EMM. If we set $\nu_j = 1$ and $\delta(x_i|\Omega_j) = 1$, then our method is similar to the WMM. When $\nu_j = 1$, $\gamma_j = 2$, and $\delta(x_i|\Omega_j) = 1$ the proposed method is similar to the RMM in ([31]- [32]). And our method is similar to the EWMM [8] when $\delta(x_i|\Omega_j) = 1$. Presently, we contrasted our technique and BEMM in ([33]- [34]), and in the event that we put $\gamma_j = 1$, $\nu_j = 1$and $\delta(x_i|\Omega_j) = \delta(x_i|\Omega_k)$: $\forall j,\ k = \{1,2,3,...,K\}$, our strategy is like the BEMM. Essentially, our strategy is like the double truncated Weibull mixture model (BWMM) [35] when we put $\nu_j = 1$

and $\delta(x_i|\Omega_j) = \delta(x_i|\Omega_k)$: $\forall j,\ k = \{1,2,3,...,K\}$. Accordingly, it could be said that the fundamental model of the proposed technique is a speculation of the EMM, WMM, RMM, GEMM, BEMM, BWMM, BRMM [36], and BGEMM [37] models. The special cases of the proposed method see Table 1. Given the log-likelihood function in (2.8), the following goal is to upgrade the parameter set keeping in mind the end goal to maximize this log-likelihood function.

3. Maximizing the log-likelihood function

As yet, the discussion has focused on Y_{ij} in (2.4) for showing the fundamental distributions. With a particular finished objective to adjust the parameters $\Theta = \{\rho_j, \mu_j, \beta_j, \nu_j, \gamma_j\}$, we need to maximize the likelihood function in (2.8). For all cases, the strategy is the maximum likelihood method, based in a numerical scheme. The difference lies rather in the numerical scheme (direct estimation or Newton-Raphson method), so remembering the finished objective to present accommodatingly, we subdivide this range into three subsections.

3.1. **Mean estimation.**

Following the logarithm is a monotonically increasing function, it is more advantageous to maximize the likelihood $L(\Theta)$ in (2.8). The variable ω_{ij} is defined as

$$\omega_{ij} = \frac{\rho_j \mathrm{Y}_{ij}(x_i|\theta_j)}{\sum_{m=1}^{K} \rho_m \mathrm{Y}_{ij}(x_i|\theta_m)} \text{ with } \sum_{j=1}^{K} \omega_{ij} = 1. \tag{3.1}$$

To maximize this function in (2.8), we consider the derivation of the function $L(\Theta)$ with the means μ_j at the $(t+1)$ iteration step. We have

$$\begin{aligned}
\frac{\partial L}{\partial \mu_j} &= \sum_{i=1}^{N} \frac{\omega_{ij}}{\mathrm{Y}_{ij}} \frac{\mathrm{Y}_{ij}}{\partial \mu_j} \\
&= \sum_{i=1}^{N} \omega_{ij} \Big\{ |x_i - \mu_j|^{-1} \mathrm{sign}(\mu_j - x_i) \Big(\gamma_j - 1 - \beta_j \gamma_j |x_i - \mu_j|^{\gamma_j} + \\
&(\nu_j - 1)\beta_j \gamma_j |x_i - \mu_j|^{\gamma_j} \exp(-\beta_j |x_i - \mu_j|^{\gamma_j}) (1 - \exp(-\beta_j |x_i - \mu_j|^{\gamma_j}))^{-1} \Big) - \\
&\frac{1}{\int_{\partial_j} T(x|\theta_j) dx} \Big[\int_{\partial_j} |x - \mu_j|^{-1} \mathrm{sign}(\mu_j - x) \Big(\gamma_j - 1 - \beta_j \gamma_j |x - \mu_j|^{\gamma_j} + \\
&(\nu_j - 1)\beta_j \gamma_j |x - \mu_j|^{\gamma_j} \exp(-\beta_j |x - \mu_j|^{\gamma_j}) (1 - \exp(-\beta_j |x - \mu_j|^{\gamma_j}))^{-1} \Big) T(x|\theta_j) dx \Big] \Big\},
\end{aligned} \tag{3.2}$$

where $\mathrm{sign}(x)$ is equal to 1, if $x \geq 0$ and -1, otherwise. Notice that in (3.2), the term

$$\begin{aligned}
&\int_{\partial_j} |x - \mu_j|^{-1} \mathrm{sign}(\mu_j - x) \Big(\gamma_j - 1 - \beta_j \gamma_j |x - \mu_j|^{\gamma_j} + \\
&(\nu_j - 1)\beta_j \gamma_j |x - \mu_j|^{\gamma_j} \exp(-\beta_j |x - \mu_j|^{\gamma_j}) (1 - \exp(-\beta_j |x - \mu_j|^{\gamma_j}))^{-1} \Big) T(x|\theta_j) dx,
\end{aligned}$$

is the expectation of the function

$$|x-\mu_j|^{-1}\text{sign}(\mu_j-x)\Big(\gamma_j-1-\beta_j\gamma_j|x-\mu_j|^{\gamma_j}+$$
$$(\nu_j-1)\beta_j\gamma_j|x-\mu_j|^{\gamma_j}\exp(-\beta_j|x-\mu_j|^{\gamma_j})(1-\exp(-\beta_j|x-\mu_j|^{\gamma_j}))^{-1}\Big),$$

under the probability distribution $T(x|\theta_j)$. At that point, this desire can be approximated as ([16] and [28])

$$\int_{\partial_j} T(x|\theta_j)dx \approx \frac{1}{M}\sum_{m=1}^{M}\delta(v_{m_j}/\Omega_j), \tag{3.3}$$

$$\begin{aligned}&\int_{\partial_j}|x-\mu_j|^{-1}\text{sign}(\mu_j-x)\Big(\gamma_j-1-\beta_j\gamma_j|x-\mu_j|^{\gamma_j}+\\&(\nu_j-1)\beta_j\gamma_j|x-\mu_j|^{\gamma_j}\exp(-\beta_j|x-\mu_j|^{\gamma_j})(1-\exp(-\beta_j|x-\mu_j|^{\gamma_j}))^{-1}\Big)T(x|\theta_j)dx\approx\\&\frac{1}{M}\sum_{m=1}^{M}\delta(v_{m_j}|\Omega_j)|v_{m_j}-\mu_j^{(t)}|^{-1}\text{sign}(\mu_j^{(t)}-v_{m_j})\Big(\gamma_j^{(t)}-1-\beta_j^{(t)}\gamma_j^{(t)}|v_{m_j}-\mu_j^{(t)}|^{\gamma_j^{(t)}}+\\&(\nu_j^{(t)}-1)\beta_j^{(t)}\gamma_j^{(t)}|v_{m_j}-\mu_j^{(t)}|^{\gamma_j^{(t)}}\exp(-\beta_j^{(t)}|v_{m_j}-\mu_j^{(t)}|^{\gamma_j^{(t)}})(1-\exp(-\beta_j^{(t)}|v_{m_j}-\mu_j^{(t)}|^{\gamma_j^{(t)}}))^{-1}\Big)\end{aligned} \tag{3.4}$$

such that $v_{m_j}\sim T(x|\theta_j^{(t)})$ indicates the random variable that is drawn from the probability distribution $T(x|\theta_j^{(t)})$, and M is the number of random variables v_{mj}. Note that M is an extensive whole number worth. We utilize $M=10^6$ for our experiments.
From (3.3) and (3.4), $\dfrac{\partial L}{\partial\mu_j}$ in (3.2) has the following form

$$\begin{aligned}\frac{\partial L}{\partial\mu_j}\approx\sum_{i=1}^{N}\omega_{ij}\Big\{&|x_i-\mu_j|^{-1}\text{sign}(\mu_j-x_i)\Big(\gamma_j-1-\beta_j\gamma_j|x_i-\mu_j|^{\gamma_j}+\\&(\nu_j-1)\beta_j\gamma_j|x_i-\mu_j|^{\gamma_j}\exp(-\beta_j|x_i-\mu_j|^{\gamma_j})(1-\exp(-\beta_j|x_i-\mu_j|^{\gamma_j}))^{-1}\Big)+R_j\Big\},\end{aligned} \tag{3.5}$$

where

$$\begin{aligned}R_j=&\frac{1}{\sum_{m=1}^{M}\delta(v_{m_j}/\Omega_j)}\sum_{m=1}^{M}\delta(v_{m_j}/\Omega_j)|v_{m_j}-\mu_j^{(t)}|^{-1}\text{sign}(\mu_j^{(t)}-v_{m_j})\Big[\gamma_j^{(t)}-1-\beta_j^{(t)}\gamma_j^{(t)}|v_{m_j}-\mu_j^{(t)}|^{\gamma_j^{(t)}}+\\&(\nu_j^{(t)}-1)\beta_j^{(t)}\gamma_j^{(t)}|v_{m_j}-\mu_j^{(t)}|^{\gamma_j^{(t)}}\exp(-\beta_j^{(t)}|v_{m_j}-\mu_j^{(t)}|^{\gamma_j^{(t)}})(1-\exp(-\beta_j^{(t)}|v_{m_j}-\mu_j^{(t)}|^{\gamma_j^{(t)}}))^{-1}\Big].\end{aligned} \tag{3.6}$$

Using the theory of robust statistics ([17], [38]), any estimate U is defined by an implicit equation:

$$\sum_{i=1}^{N}f(x_i-U)=0\Rightarrow\varrho_i=\frac{f(x_i-U)}{x_i-U}\text{ and }U=\frac{\sum_{i=1}^{N}\varrho_i x_i}{\sum_{i=1}^{N}\omega_i}. \tag{3.7}$$

Now we can apply (3.7) to the $\dfrac{\partial L}{\partial\mu_j}$ in (3.5), the solution of $\dfrac{\partial L}{\partial\mu_j}=0$ yields the solutions μ_j of at the $(t+1)$ step:

$$\mu_j^{(t+1)} = \frac{\sum_{i=1}^{N} \omega_{ij}^{(t)} \Big\{ |x_i - \mu_j^{(t)}|^{-2} x_i E_{ij} + R_j \Big\}}{\sum_{i=1}^{N} \omega_{ij}^{(t)} |x_i - \mu_j^{(t)}|^{-2} E_{ij}}, \tag{3.8}$$

where

$$E_{ij} = \Big(\gamma_j - 1 - \beta_j \gamma_j |x_i - \mu_j|^{\gamma_j} + (\nu_j - 1)\beta_j \gamma_j |x_i - \mu_j|^{\gamma_j} \exp(-\beta_j |x_i - \mu_j|^{\gamma_j}) (1 - \exp(-\beta_j |x_i - \mu_j|^{\gamma_j}))^{-1} \Big).$$

3.2. **Shape, scale and power parameters estimation.** The accompanying step is to redesign the examination of the parameter ν_j. This incorporates holding interchange parameters settled and improving the examination of ν_j using the Newton Raphson method [[13], [18], [39]]. Every cycle requires the first and second derivatives of the objective function regarding the parameter ν_j

$$\nu_j^{(t+1)} = \nu_j^{(t)} - \frac{\frac{\partial L}{\partial \nu_j}}{\frac{\partial^2 L}{\partial \nu_j^2} + \varepsilon} \Big|_{\nu_j = \nu_j^{(t)}}, \tag{3.9}$$

where ε is a scaling element. The derivative of the function $L(\Theta)$ regarding ν_j is given by

$$\frac{\partial L}{\partial \nu_j} = \sum_{i=1}^{N} \frac{\omega_{ij}}{\Upsilon_{ij}} \frac{\Upsilon_{ij}}{\partial \nu_j} = \sum_{i=1}^{N} \omega_{ij} \Big\{ \frac{1}{\nu_j} + \log\Big(1 - \exp(-\beta_j |x_i - \mu_j|^{\gamma_j})\Big) - \frac{\int_{\partial_j} \Big[\frac{1}{\nu_j} + \log\Big(1 - \exp(-\beta_j |x - \mu_j|^{\gamma_j})\Big) \Big] T(x|\theta_j) dx}{\int_{\partial_j} T(x|\theta_j) dx} \Big\}. \tag{3.10}$$

Using (3.3) and (3.4), the term $\frac{\partial L}{\partial \nu_j}$ can be approximated as

$$\frac{\partial L}{\partial \nu_j}\Big|_{\nu_j = \nu_j^{(t)}} \approx \sum_{i=1}^{N} \omega_{ij} \Big\{ \frac{1}{\nu_j} + \log\Big(1 - \exp(-\beta_j |x_i - \mu_j|^{\gamma_j})\Big) - \frac{\sum_{m=1}^{M} \delta(v_{m_j}|\Omega_j) \Big(\frac{1}{\nu_j^{(t)}} + \log\Big(1 - \exp(-\beta_j^{(t)} |v_{m_j} - \mu_j^{(t)}|^{\gamma_j^{(t)}})\Big)\Big)}{\sum_{m=1}^{M} \delta(v_{m_j}|\Omega_j)} \Big\}. \tag{3.11}$$

The term $\frac{\partial^2 L}{\partial \nu_j^2}$ is given by

$$\frac{\partial^2 L}{\partial \nu_j^2} = \sum_{i=1}^{N} \Big[\omega_{ij}(1 - \omega_{ij}) \Big\{ \frac{1}{\nu_j} + \log\Big(1 - \exp(-\beta_j |x_i - \mu_j|^{\gamma_j})\Big) - \frac{\int_{\partial_j} \Big\{ \frac{1}{\nu_j} + \log\Big(1 - \exp(-\beta_j |x - \mu_j|^{\gamma_j})\Big) \Big\} T(x|\theta_j) dx}{\int_{\partial_j} T(x|\theta_j) dx} \Big\}^2 + \tag{3.12}$$

$$\omega_{ij}\Big\{\frac{-1}{\nu_j^2}+\frac{(\int_{\partial_j}T(x|\theta_j)f dx)^2}{(\int_{\partial_j}T(x|\theta_j)dx)^2}-\frac{\int_{\partial_j}(\frac{-1}{\nu_j^2}+f^2)T(x|\theta_j)dx}{\int_{\partial_j}T(x|\theta_j)dx}\Big\}\Big],$$

where

$$f(x_i|\theta_j)=\frac{1}{\nu_j}+\log\Big(1-\exp(-\beta_j|x_i-\mu_j|^{\gamma_j})\Big). \tag{3.13}$$

Also by using (3.3) and (3.4), the term $\dfrac{\partial^2 L}{\partial \nu_j^2}$ can be approximated as

$$\begin{aligned}\frac{\partial^2 L}{\partial \nu_j^2}\Big|_{\eta_j=\eta_j^{(t)}} \approx \sum_{i=1}^{N}\Big[\omega_{ij}^{(t)}(1-\omega_{ij}^{(t)})\Big\{\frac{1}{\nu_j^{(t)}}+\log\Big(1-\exp(-\beta_j^{(t)}|x_i-\mu_j^{(t)}|^{\gamma_j^{(t)}})\Big)-\\ \frac{\sum_{m=1}^{M}\delta(v_{m_j}|\Omega_j)\Big\{\frac{1}{\nu_j^{(t)}}+\log\Big(1-\exp(-\beta_j^{(t)}|v_{m_j}-\mu_j^{(t)}|^{\gamma_j^{(t)}})\Big)\Big\}}{\sum_{m=1}^{M}\delta(v_{m_j}|\Omega_j)}\Big\}^2+\\ \omega_{ij}^{(t)}\Big\{\frac{-1}{(\nu_j^{(t)})^2}+\frac{(\sum_{m=1}^{M}\delta(v_{m_j}|\Omega_j)(f^{(t)}))^2}{(\sum_{m=1}^{M}\delta(v_{m_j}|\Omega_j))^2}-\frac{\sum_{m=1}^{M}\delta(v_{m_j}|\Omega_j)(\frac{-1}{(\nu_j^{(t)})^2})+(f^{(t)})^2)}{\sum_{m=1}^{M}\delta(v_{m_j}|\Omega_j)}\Big\}\Big],\end{aligned} \tag{3.14}$$

where

$$f^{(t)}=\frac{1}{\nu_j^{(t)}}+\log\Big(1-\exp(-\beta_j^{(t)}|v_{m_j}-\mu_j^{(t)}|^{\gamma_j^{(t)}})\Big). \tag{3.15}$$

For scale parameter estimation β_j by using the Newton Raphson method, we have

$$\beta_j^{(t+1)}=\beta_j^{(t)}-\frac{\frac{\partial L}{\partial \beta_j}}{\frac{\partial^2 L}{\partial \beta_j^2}+\varepsilon}\Big|_{\beta_j=\beta_j^{(t)}}. \tag{3.16}$$

The derivative of the function $L(\Theta)$ with respect to β_j is given by

$$\begin{aligned}\frac{\partial L}{\partial \beta_j}&=\sum_{i=1}^{N}\frac{\omega_{ij}}{\Upsilon_{ij}}\frac{\Upsilon_{ij}}{\partial \beta_j}\\ &=\sum_{i=1}^{N}\omega_{ij}\Big\{g(x_i|\theta_j)-\frac{\int_{\partial_j}g(x|\theta_j)T(x|\theta_j)dx}{\int_{\partial_j}T(x|\theta_j)dx}\Big\},\end{aligned} \tag{3.17}$$

where

$$g(x_i|\theta_j)=\frac{1}{\beta_j}-|x_i-\mu_j|^{\gamma_j}+(\nu_j-1)|x_i-\mu_j|^{\gamma_j}\exp(-\beta_j|x_i-\mu_j|^{\gamma_j})(1-\exp(-\beta_j|x_i-\mu_j|^{\gamma_j}))^{-1}. \tag{3.18}$$

Like to (3.3) and (3.4), the term $\dfrac{\partial L}{\partial \beta_j}$ can be approximated as

$$\frac{\partial L}{\partial \beta_j}\Big|_{\beta_j=\beta_j^{(t)}}\approx\sum_{i=1}^{N}\omega_{ij}^{(t)}\Big\{g(x_i|\theta_j^{(t)})-\frac{\sum_{m=1}^{M}\delta(v_{m_j}|\Omega_j)g(v_{m_j}|\theta_j^{(t)})}{\sum_{m=1}^{M}\delta(v_{m_j}|\Omega_j)}\Big\}. \tag{3.19}$$

The calculation of the terms $\frac{\partial^2 L}{\partial \beta_j^2}$ is obtained as

$$\begin{aligned}\frac{\partial^2 L}{\partial \beta_j^2} = \sum_{i=1}^{N}\Big[\omega_{ij}(1-\omega_{ij})\Big\{g(x_i|\theta_j) - \frac{\int_{\partial_j} g(x|\theta_j)T(x|\theta_j)dx}{\int_{\partial_j} T(x|\theta_j)dx}\Big\}^2 + \\ \omega_{ij}\Big\{\frac{\partial g(x_i|\theta_j)}{\partial \beta_j} + \frac{(\int_{\partial_j} T(x|\theta_j)g(x|\theta_j)dx)^2}{(\int_{\partial_j} T(x|\theta_j)dx)^2} - \frac{\int_{\partial_j}(\frac{\partial g(x|\theta_j)}{\partial \beta_j} + g^2(x|\theta_j))T(x|\theta_j)dx}{\int_{\partial_j} T(x|\theta_j)dx}\Big\}\Big],\end{aligned} \tag{3.20}$$

where

$$\frac{\partial g}{\partial \beta_j} = \frac{-1}{\beta_j^2} - (\nu_j - 1)|x_i - \mu_j|^{2\gamma_j}\exp(-\beta_j|x_i-\mu_j|^{\gamma_j})(1-\exp(-\beta_j|x_i-\mu_j|^{\gamma_j}))^{-2}.$$

Similar to (3.3) and (3.4), the term $\frac{\partial^2 L}{\partial \beta_j^2}$ can be approximated as

$$\begin{aligned}\frac{\partial^2 L}{\partial \beta_j^2}\Big|_{\beta_j=\beta_j^{(t)}} \approx \sum_{i=1}^{N}\Big[\omega_{ij}^{(t)}(1-\omega_{ij}^{(t)})\Big\{g(x_i|\theta_j) - \frac{\sum_{m=1}^{M}\delta(v_{m_j}|\Omega_j)g(v_{m_j}|\theta_j)}{\sum_{m=1}^{M}\delta(v_{m_j}|\Omega_j)}\Big\}^2 + \\ \omega_{ij}^{(t)}\Big\{(\frac{\partial g(x_i|\theta_j)}{\partial \beta_j})^{(t)} + \frac{(\sum_{m=1}^{M}\delta(v_{m_j}|\Omega_j)g^{(t)}(v_{m_j}|\theta_j))^2}{(\sum_{m=1}^{M}\delta(v_{m_j}|\Omega_j))^2} - \\ \frac{\sum_{m=1}^{M}\delta(v_{m_j}|\Omega_j)((\frac{\partial g(v_{m_j}|\theta_j)}{\partial \beta_j})^{(t)} + (g^{(t)}(v_{m_j}|\theta_j))^2)}{\sum_{m=1}^{M}\delta(v_{m_j}|\Omega_j)}\Big\}\Big],\end{aligned} \tag{3.21}$$

where

$$\begin{aligned}g^{(t)} = \frac{1}{\beta_j^{(t)}} - |v_{m_j} - \mu_j^{(t)}|^{\gamma_j^{(t)}} \\ + (\nu_j^{(t)} - 1)|v_{m_j} - \mu_j^{(t)}|^{\gamma_j^{(t)}}\exp(-\beta_j^{(t)}|v_{m_j} - \mu_j^{(t)}|^{\gamma_j^{(t)}})(1-\exp(-\beta_j^{(t)}|v_{m_j} - \mu_j^{(t)}|^{\gamma_j^{(t)}}))^{-1},\end{aligned} \tag{3.22}$$

and

$$(\frac{\partial g(x_i|\theta_j)}{\partial \beta_j})^{(t)} = \frac{-1}{(\beta_j^2)^{(t)}} - (\nu_j^{(t)} - 1)|x_i - \mu_j^{(t)}|^{2\gamma_j^{(t)}}\exp(-\beta_j^{(t)}|x_i - \mu_j^{(t)}|^{\gamma_j^{(t)}})(1-\exp(-\beta_j^{(t)}|x_i - \mu_j^{(t)}|^{\gamma_j^{(t)}}))^{-2}. \tag{3.23}$$

The power parameter estimation γ_j by Newton Raphson technique is

$$\gamma_j^{(t+1)} = \gamma_j^{(t)} - \frac{\frac{\partial L}{\partial \gamma_j}}{\frac{\partial^2 L}{\partial \gamma_j^2} + \varepsilon}\Big|_{\gamma_j=\gamma_j^{(t)}}. \tag{3.24}$$

The derivative of the function $L(\Theta)$ with respect to γ_j is given by

$$\frac{\partial L}{\partial \gamma_j} = \sum_{i=1}^{N}\frac{\omega_{ij}}{\Upsilon_{ij}}\frac{\Upsilon_{ij}}{\partial \gamma_j} = \sum_{i=1}^{N}\omega_{ij}\Big\{h(x_i|\theta_j) - \frac{\int_{\partial_j} h(x|\theta_j)T(x|\theta_j)dx}{\int_{\partial_j} T(x|\theta_j)dx}\Big\}, \tag{3.25}$$

where

$$h(x_i|\theta_j) = \frac{1}{\gamma_j} + \log|x_i-\mu_j| - \beta_j|x_i-\mu_j|^{\gamma_j}\log|x_i-\mu_j| \times \left[1-(\nu_j-1)\exp(-\beta_j|x_i-\mu_j|^{\gamma_j})(1-\exp(-\beta_j|x_i-\mu_j|^{\gamma_j}))^{-1}\right]. \tag{3.26}$$

Such (3.3) and (3.4), the term $\frac{\partial L}{\partial \gamma_j}$ can be approximated as

$$\frac{\partial L}{\partial \gamma_j}\Big|_{\gamma_j=\gamma_j^{(t)}} \approx \sum_{i=1}^{N}\omega_{ij}^{(t)}\Big\{h(x_i|\theta_j^{(t)}) - \frac{\sum_{m=1}^{M}\delta(v_{m_j}|\Omega_j)h(v_{m_j}|\theta_j^{(t)})}{\sum_{m=1}^{M}\delta(v_{m_j}|\Omega_j)}\Big\}. \tag{3.27}$$

The calculation of the terms $\frac{\partial^2 L}{\partial \gamma_j^2}$ is obtained as

$$\frac{\partial^2 L}{\partial \gamma_j^2} = \sum_{i=1}^{N}\Big[\omega_{ij}(1-\omega_{ij})\Big\{h(x_i|\theta_j) - \frac{\int_{\partial_j}h(x|\theta_j)T(x|\theta_j)dx}{\int_{\partial_j}T(x|\theta_j)dx}\Big\}^2 + \omega_{ij}\Big\{\frac{\partial h(x_i|\theta_j)}{\partial\gamma_j} + \frac{(\int_{\partial_j}T(x|\theta_j)h(x|\theta_j)dx)^2}{(\int_{\partial_j}T(x|\theta_j)dx)^2} - \frac{\int_{\partial_j}(\frac{\partial h(x|\theta_j)}{\partial\gamma_j}+h^2(x|\theta_j))T(x|\theta_j)dx}{\int_{\partial_j}T(x|\theta_j)dx}\Big\}\Big], \tag{3.28}$$

where

$$\frac{\partial h(x_i|\theta_j)}{\partial\gamma_j} = \frac{-1}{\gamma_j^2} - \beta_j|x_i-\mu_j|^{\gamma_j}\log^2|x_i-\mu_j| + \beta_j(\nu_j-1)|x_i-\mu_j|^{\gamma_j}\exp(-2\beta_j|x_i-\mu_j|^{\gamma_j})(1-\exp(-\beta_j|x_i-\mu_j|^{\gamma_j}))^{-2}\log^2|x_i-\mu_j| \times \Big[-\beta_j|x_i-\mu_j|^{\gamma_j}\exp(\beta_j|x_i-\mu_j|^{\gamma_j}) + \exp(\beta_j|x_i-\mu_j|^{\gamma_j}) - 1\Big].$$

Similar to (3.3) and (3.4), the term $\frac{\partial^2 L}{\partial \gamma_j^2}$ can be approximated as

$$\frac{\partial^2 L}{\partial \gamma_j^2}\Big|_{\gamma_j=\gamma_j^{(t)}} \approx \sum_{i=1}^{N}\Big[\omega_{ij}^{(t)}(1-\omega_{ij}^{(t)})\Big\{h(x_i|\theta_j) - \frac{\sum_{m=1}^{M}\delta(v_{m_j}|\Omega_j)h(v_{m_j}|\theta_j)}{\sum_{m=1}^{M}\delta(v_{m_j}|\Omega_j)}\Big\}^2 + \omega_{ij}^{(t)}\Big\{(\frac{\partial h(x_i|\theta_j)}{\partial\gamma_j})^{(t)} + \frac{(\sum_{m=1}^{M}\delta(v_{m_j}|\Omega_j)h^{(t)}(v_{m_j}|\theta_j))^2}{(\sum_{m=1}^{M}\delta(v_{m_j}|\Omega_j))^2} - \frac{\sum_{m=1}^{M}\delta(v_{m_j}|\Omega_j)((\frac{\partial h(v_{m_j}|\theta_j)}{\partial\gamma_j})^{(t)} + (h^{(t)}(v_{m_j}|\theta_j))^2)}{\sum_{m=1}^{M}\delta(v_{m_j}|\Omega_j)}\Big\}\Big], \tag{3.29}$$

where

$$h^{(t)}(v_{m_j}|\theta_j) = \frac{1}{\gamma_j^{(t)}} + \log|v_{m_j}-\mu_j^{(t)}| - \beta_j^{(t)}|v_{m_j}-\mu_j^{(t)}|^{\gamma_j^{(t)}}\log|v_{m_j}-\mu_j^{(t)}| \times \Big[1-(\nu_j^{(t)}-1)\exp(-\beta_j^{(t)}|v_{m_j}-\mu_j^{(t)}|^{\gamma_j^{(t)}})(1-\exp(-\beta_j^{(t)}|v_{m_j}-\mu_j^{(t)}|^{\gamma_j^{(t)}}))^{-1}\Big], \tag{3.30}$$

and

$$(\frac{\partial h(v_{m_j}|\theta_j)}{\partial \gamma_j})^{(t)} = \frac{-1}{(\gamma_j^{(t)})^2} - \beta_j^{(t)}|x_i - \mu_j^{(t)}|^{\gamma_j^{(t)}} \log^2|v_{m_j} - \mu_j^{(t)}| +$$
$$\beta_j^{(t)}(\nu_j^{(t)} - 1)|v_{m_j} - \mu_j^{(t)}|^{\gamma_j^{(t)}} \exp(-2\beta_j^{(t)}|v_{m_j} - \mu_j^{(t)}|^{\gamma_j^{(t)}})(1 - \exp(-\beta_j^{(t)}|v_{m_j} - \mu_j^{(t)}|^{\gamma_j^{(t)}}))^{-2} \log^2|v_{m_j} - \mu_j^{(t)}|$$
$$\times\Big[-\beta_j^{(t)}|v_{m_j} - \mu_j^{(t)}|^{\gamma_j^{(t)}} \exp(\beta_j^{(t)}|v_{m_j} - \mu_j^{(t)}|^{\gamma_j^{(t)}}) + \exp(\beta_j^{(t)}|v_{m_j} - \mu_j^{(t)}|^{\gamma_j^{(t)}}) - 1\Big]. \tag{3.31}$$

3.3. **Prior probability estimation and the algorithm.** In this part is to update the estimate of the prior probability ρ_j. Note that the prior probability ρ_j should satisfy the constraints in (3.1). The constraint $\sum_{j=1}^{K} \rho_j = 1$ enables

$$\rho_j^{(t+1)} = \frac{1}{N}\sum_{i=1}^{N} \omega_{ij}^{(t)}. \tag{3.32}$$

So far, the discussion has focused on estimating $\Theta(\rho_j, \mu_j, \beta_j, \nu_j, \gamma_j)$ of the model. The various steps of the proposed mixture model can be summarized as follows

Step 1: Initialize the parameters $\Theta(\rho_j, \mu_j, \beta_j, \nu_j, \gamma_j)$. + The initialization of the parameters $\Theta(\rho_j, \mu_j, \beta_j)$ in our method are the same as that of BGGMM [37]. The initial value of γ_j is set to 2 and the initial value of ν_j is set to 1, for the simulation data. The initial value of γ_j is set to 1 and the initial value of ν_j is set to 2, for the real data, since for the real data in many of the image processing examples the wavelet histogram fitting is approximately follows Gaussian distribution.

Step 2: Evaluate the variables ω_{ij} in (3.1).

Step 3: Re-estimate the parameters $\Theta(\rho_j, \mu_j, \beta_j, \nu_j, \gamma_j)$, where the most common value of scaling parameter ε is 10^{-20} for our experiments.

+ Update the means by using (3.8).

+Update the parameter ν_j in (3.9).

+Update the parameter β_j in (3.16).

+Update the parameter γ_j in (3.24).

+Update the prior probability ρ_j in (3.32).

Step 4: Evaluate the function in (2.8) and check for the convergence of either the function, or the parameter values. In the event that the convergence is not fulfilled, then go to step 2.

Looking at the mathematical expressions of the parameter learning of $\rho_j, \mu_j, \beta_j, \nu_j, \gamma_j$, we can see that our methodology, which is to maximize the higher bound on the data log-likelihood function, offers a closed form M-step with computational intricacy like that of the standard EM algorithm. In any case, for the standard EM algorithm, so as to estimate the parameter γ_j, we have to set $\frac{\partial L(\Theta)}{\partial \gamma_j}$ equal to zero and acquire the parameters γ_j at the cycle $(t+1)$ step. Shockingly, as a result of the complexity of equations $L(\Theta)$ in (2.8), there are no closed form overhaul mathematical statements for parameter by embracing the standard EM algorithm. Conversely with the standard

EM algorithm, our methodology can make it simple to evaluate the parameters ν_j, β_j and γ_j from perceptions by maximizing the higher bound on the data log-likelihood function as appeared in (3.9), (3.16) and (3.24) separately. In the following segment, we will exhibit the robustness, accuracy, and effectiveness of the proposed model, as compared with other methodologies.

4. Experiments

We show the execution of the proposed technique in different examinations. The execution of BEWMM is contrasted with the WMM [25], RMM [31], EMM [23], EWMM [21], BWMM [35], BRMM [36], GEMM [13], and BGEMM [37] all with their double truncated forms. These strategies are instated by the K-mean algorithm like the introduction of the proposed technique. To gauge the fitting precision of every model, we utilize the goodness of-fit measurement value χ^2, which is figured as takes after [13]:

$$\chi^2 = \sum_x \frac{[O(x) - E(x)]^2}{E(x)}, \tag{4.1}$$

where $O(x)$, and $E(x)$ speak to the observational and expected frequencies, individually, for the watched information. Note that, all the thought about strategies were rehashed 10 runs and the normal estimation of the measurement qualities is recorded. Also we use information criterions such as Akaike information criterion (AIC) [40], correct Akaike information criterion (CAIC) [41] and Bayesian information criterion (BIC) [42] to complement our results. In the main test the histogram of the watched information are displayed in Fig.1 (a) and (b), where the watched information are in the interval (- 0.8, 0.6). We generate 90000 random numbers from BEWMM with parameters $\rho_1 = \frac{5291}{90000}$, $\rho_2 = \frac{37084}{90000}$, $\gamma_1 = 0.87$, $\gamma_2 = 1.67$, $\mu_1 = -0.2$, $\mu_2 = 0.3$, $\beta_1 = 15.4084$, $\beta_2 = 55.8645$, $\nu_1 = 2.3$, and $\nu_2 = 1.2$. In this test, the quantity of segments for all thought about techniques is allocated an estimation of 2 ($K = 2$). In Fig. 2(b), the WMM strategy is extremely poor and the tail of the Weibull distribution is taller than required, with $\chi^2 = 411.23$. The GEMM, RMM, and EWMM strategies enhance the outcome, with $\chi^2 = 15.09$, $\chi^2 = 12.87$, and $\chi^2 = 12.73$, individually. Contrasted with WMM, GEMM, RMM, and EWMM, we find that BEWMM is the most powerful and has the least $\chi^2 = 12.56$. In the second examination the histogram of the watched information are exhibited in Fig.2 (a) and (b-g), where the watched information are in the interval (0.1, 0.5). In this trial, the quantity of parts for all thought about techniques is appointed an estimation of 1($K = 1$). We generate 47524 random numbers from BEWMM with parameters $\gamma_1 = 1.67$, $\mu_1 = 0.32$, $\beta_1 = 55.8645$, and $\nu_1 = 1.2$. In Fig. 2(b-g), the WMM is exceptionally poor and the tail of the Weibull distribution is taller than required, with $\chi^2 = 3299.2108$. Also for the models BWMM ($\chi^2 = 3276.5167$) with taller tail, EMM ($\chi^2 = 1429.2013$) and BEMM ($\chi^2 = 1413.0125$) are middle taller, GEMM ($\chi^2 = 33.6702$), BGEMM ($\chi^2 = 33.4213$), BMM ($\chi^2 = 32.06$), EWMM ($\chi^2 = 28.77$), RMM ($\chi^2 = 29.23$), and BRMM ($\chi^2 = 29$). We find that BEWMM is the most powerful and has the least $\chi^2 = 28.33$. This shows, to fit the information, the proposed approach utilizes less mind boggling models than the BWMM approaches. This perspective is of noticeable significance

for image coding and compression applications ([43], [44]). In the following investigation of Fig. 3, we will clarify in subtle element why the execution of the proposed technique is superior to that of these strategies. In this test, two illustrations with the histogram of the watched information, where the watched information are in the interval $(-0.5, -0.1)$. We generate 47524 random numbers from BEWMM with parameters $K = 1$, $\gamma_1 = 1.5385$, $\mu_1 = -0.3$, $\beta_1 = 44.8662$, and $\nu_1 = 1.3$. Fig. 3 (b) and (c) demonstrate the aftereffects of BГMM, WMM, BWMM, BRMM, BGGMM, and our technique, separately. As demonstrated, the techniques with the supporting locales (WMM, BWMM, and BEMM) with ($\chi^2 = 3201$), ($\chi^2 = 3198$), and ($\chi^2 = 1215$) respectively are extremely poor, where the tail of the double truncated Weibull distribution and the Weibull distribution are taller than other models. the BEMM model ($\chi^2 = 1413.0125$) is middle taller. The GEMM ($\chi^2 = 33.2109$), BGEMM ($\chi^2 = 32.9183$), EWMM ($\chi^2 = 28.32$), RMM ($\chi^2 = 28.92$), and BRMM ($\chi^2 = 28.83$) techniques enhance the outcome. In this analysis, the BEMM is not sufficiently adaptable to fit the state of the information. Contrasting these methodologies, we find that BEWMM ($\chi^2 = 28.05$) is the most powerful. In correlation, the precision of the goodness-of-fit measurement esteem got by utilizing our strategy is exceptionally high. As said over, the fundamental model of the proposed technique is a speculation of the BGEMM, GEMM, WMM, BWMM, RMM, BRMM, EMM, EWMM and BEMM models. In the fourth examination the histogram of the watched information are exhibited in Fig.4 (a) and (b-c), where the watched information are in the interval (-0.8, 0.6). We generate 90000 random numbers from BEWMM with parameters $\rho_1 = \frac{5291}{90000}$, $\rho_2 = \frac{37084}{90000}$, $\gamma_1 = 0.87$, $\gamma_2 = 0.83$, $\mu_1 = -0.2$, $\mu_2 = 0.3$, $\beta_1 = 15.4084$, $\beta_2 = 14.6282$, $\nu_1 = 2.3$, and $\nu_2 = 2.4$. In this trial, the quantity of parts for all thought about techniques is appointed an estimation of $2(K = 2)$. In Fig. 4(b-c), the WMM is exceptionally poor with ($\chi^2 = 1512.03$), where the tail of the Weibull distribution is taller than other models, after that the tails of EMM and BEMM models are in middle tall. Also for the models EMM ($\chi^2 = 632$) and BEMM ($\chi^2 = 627$) have some poorness. The models GEMM ($\chi^2 = 147.83$), and EWMM ($\chi^2 = 143.02$) are good for some extent. We find that BEWMM is the most powerful and has the least ($\chi^2 = 141.35$). This shows, to fit the information, the proposed approach utilizes less mind boggling models than the WMM approaches. The wavelet approximation coefficient is an essential issue in PC vision as it assumes a noteworthy part in an extensive variety of applications. In the following test, as appeared in Fig. 5, we measure the precision of the proposed model for wavelet histogram fitting. In Fig. 5(a), we demonstrate to one genuine picture. This picture (lena) of size ($N = 90000$) is disintegrated into three high-pass subbands (CH, CV, CD) and one low-pass subband (CA). In this paper, the Daubechies channel bank (db4) is utilized. In Fig. 5(b), we demonstrate the wavelet coefficients of the high-pass subband(CH) with $K = 2$. In Fig. 5(c-g), we display the outcomes acquired by utilizing the WMM, RMM, EMM, GEMM, and BEWMM strategies, separately. As demonstrated, the tail of the Weibull distribution In Fig. 5(c) is taller than required and the tail of Rayleigh distribution In Fig. 5(e) is shorter than required. In Fig. 5(d) and 5(f), EMM, and GEMM give an all the more intense and adaptable methodology for demonstrating information contrasted with the WMM. As clear

from the outcomes, the proposed technique outflanks different strategies with the most minimal $\chi^2 = 13.69$. In Fig. 6 (a) the original image of size ($N = 63948$), in Fig. 6 (b) the estimate of the wavelet coefficients of high-pass subband (CH), (c) BWMM ($\chi^2 = 3300$), (d) BEMM ($\chi^2 = 15.07$), (e) BRMM ($\chi^2 = 621.33$), (f) BGEMM ($\chi^2 = 13.96$), and (g) BEWMM ($\chi^2 = 13.75$). The tail of the double truncated Weibull distribution in Fig. 6(c) is taller than required and the tail of double truncated Rayleigh distribution in Fig. 6(e) is shorter than required. In Fig. 7 (a) the original image of size ($N = 70917$), in Fig. 7 (b) the estimate of the wavelet coefficients (level 3, CH) with $K = 2$. In Fig. 7 (c) BWMM ($\chi^2 = 1479.23$), (d) BEMM ($\chi^2 = 143.3$), (e) RMM ($\chi^2 = 230.09$), and (f) BGEMM ($\chi^2 = 257$), the proposed strategy beats different strategies with the most minimal $\chi^2 = 130.27$. Also we have the tail of the double truncated Weibull distribution in Fig. 7(c) is taller than required and the tail of Rayleigh distribution in Fig. 7(e) is shorter than required. In Fig. 8, we explain the approximation of the wavelet coefficients (level 3, CH) with $K = 1$ for the previous image, (a) BEMM ($\chi^2 = 22.43$), and (b) BEWMM ($\chi^2 = 19.89$). In the following analysis of Fig. 9, we actualize the technique with the supporting districts (WMM, RMM, EMM, GEMM, and BEWMM) for the genuine information. In this investigation, estimate of the wavelet coefficients with $K = 1$. (a) The third unique image of size ($N = 63948$), (b) wavelet coefficients (level 2, CD), (c) WMM ($\chi^2 = 2150$), (d) EMM ($\chi^2 = 16$), (e) RMM ($\chi^2 = 2143.29$), (f) GEMM ($\chi^2 = 15.92$), and (g) BEWMM ($\chi^2 = 15.73$). As we can see, the exactness of WMM, and RMM are very poor. Be that as it may, in this genuine trial, the tails of the Weibull distribution and Rayleigh distribution are shorter than required compared to other models. the BEWMM is sufficiently adaptable to fit the state of these genuine information. To complement our results the value of log-likelihood (L), Akaike information criterion (AIC), correct Akaike information criterion (CAIC), and Bayesian information criterion (BIC) test statistic for different models are given in Tables 2-10. We see that BEWMM model is the best among those distributions since it has the smallest value of AIC, CAIC, and BIC test.

5. Conclusions

A finite mixture model taking into account the demonstrating of the probability density function, utilizing the finite exponentiated Weibull distribution of two tail, has been proposed in this paper. The upside of the proposed distribution is that it has the adaptability to fit distinctive states of watched information, for example, non-Gaussian and bounded support information. We propose a substitute methodology so as to maximize the higher bound on the information log-likelihood function with a specific end goal to gauge the model parameters. Exploratory assessment of our calculation has been led utilizing manufactured and genuine information, along these lines showing the incredible execution of the proposed model. One constraint is that the proposed strategy performs just nearby improvement. Hence, it relies on upon the beginning stage. What's more, the terrible introduction can prompt awful results. One conceivable answer for conquer this issue is to apply worldwide improvement keeping in mind the end goal to appraise the model parameters. Another restriction is that our strategy is

connected just to analyze univariate information. One conceivable expansion of this work is to utilize the limited multivariate exponentiated Weibull mixture model for investigating associated information. Another conceivable augmentation of this work for useful K setting or finding is to receive the variational Bayesian (VB) learning, Akaike information criterion (AIC), correct Akaike information criterion (CAIC), Bayesian information criterion (BIC), or minimum description length (MDL) to naturally upgrade the parameter K.

Figures

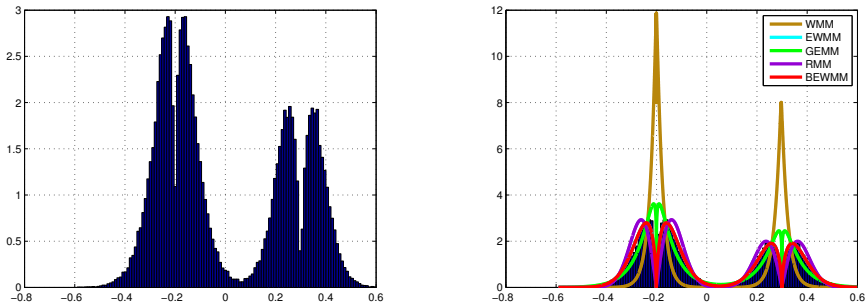

(a) (b)

FIGURE 1. The estimated histogram with $K = 2$. (a) The histogram of the observed data, (b) the estimated histogram of WMM ($\chi^2 = 411.23$), GEMM ($\chi^2 = 15.09$), RMM ($\chi^2 = 12.87$), EWMM ($\chi^2 = 12.73$), and BEWMM ($\chi^2 = 12.56$).

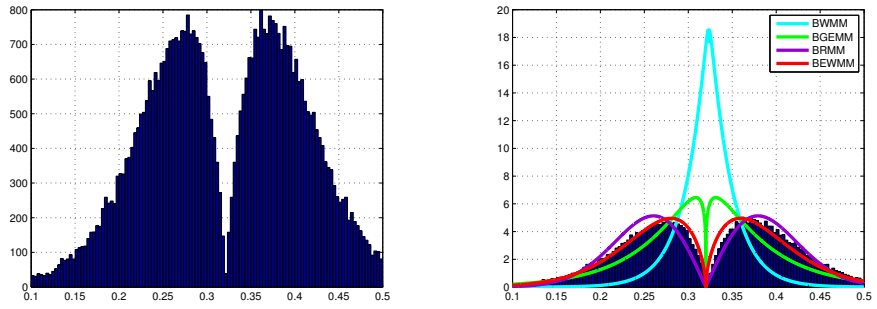

(a) (b)

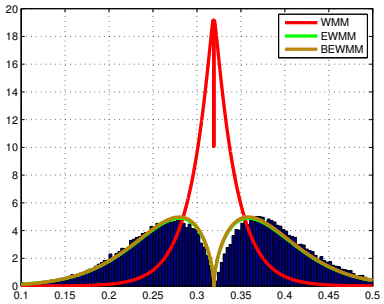

(c)

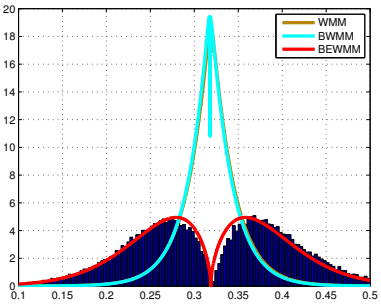

(d)

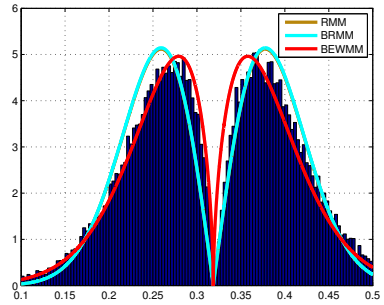

(e)

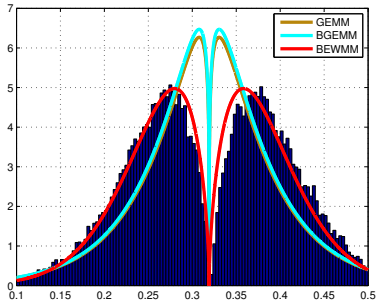

(f)

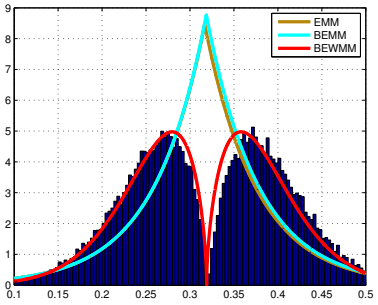

(g)

FIGURE 2. The estimated histogram with $K = 1$. (a) The histogram of the observed data, (b) the estimated histogram of BWMM ($\chi^2 = 3276.5167$), BGEMM ($\chi^2 = 33.4213$), and BRMM ($\chi^2 = 29$), (c) WMM ($\chi^2 = 3299.2108$), and EWMM ($\chi^2 = 28.77$), (e) RMM ($\chi^2 = 29.23$), (f) GEMM ($\chi^2 = 33.6702$), (g) EMM ($\chi^2 = 1429.2013$), BEMM ($\chi^2 = 1413.0125$), and BEWMM ($\chi^2 = 28.33$).

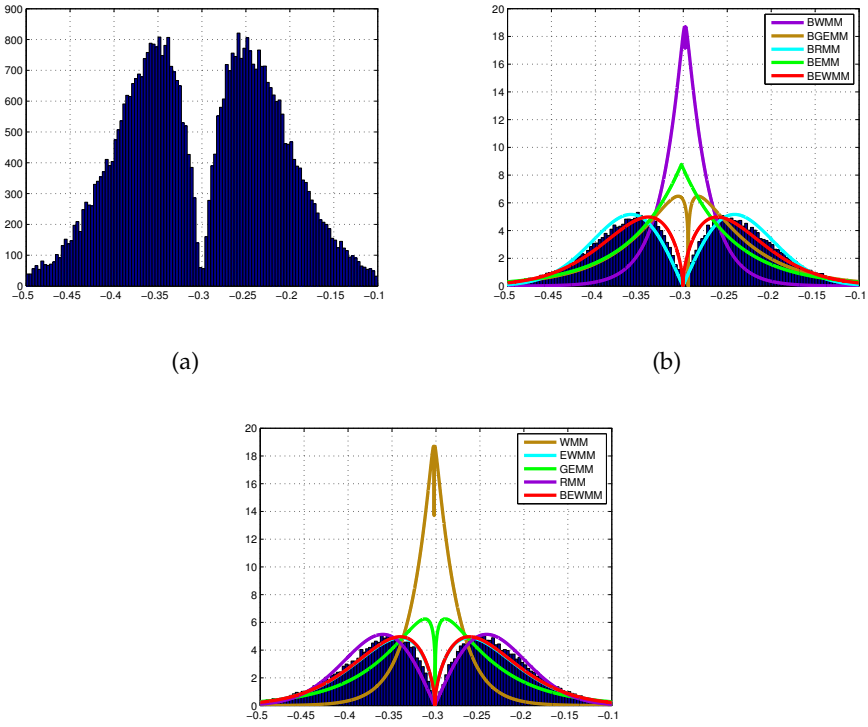

(a) (b)

(c)

FIGURE 3. The estimated histogram with $K = 1$. (a) The histogram of the observed data, (b) the estimated histogram of BWMM ($\chi^2 = 3198$), BEMM ($\chi^2 = 1215$), BGEMM ($\chi^2 = 32.9183$), and BRMM ($\chi^2 = 28.83$), (c) WMM ($\chi^2 = 3201$), GEMM ($\chi^2 = 33.2109$), EWMM ($\chi^2 = 28.32$), RMM ($\chi^2 = 28.92$), and BEWMM ($\chi^2 = 28.05$).

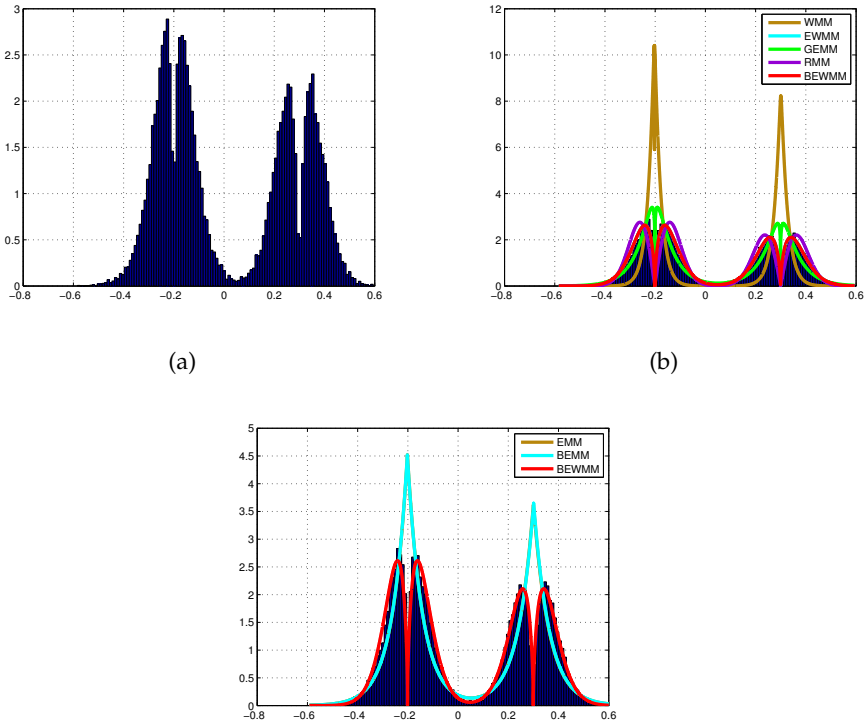

(a) (b)

(c)

FIGURE 4. The estimated histogram with $K = 2$. (a) The histogram of the observed data, (b) the estimated histogram of WMM ($\chi^2 = 1512.03$), GEMM ($\chi^2 = 147.83$), and EWMM ($\chi^2 = 143.02$), (c) EMM ($\chi^2 = 632$), BEMM ($\chi^2 = 627$), and BEWMM ($\chi^2 = 141.35$).

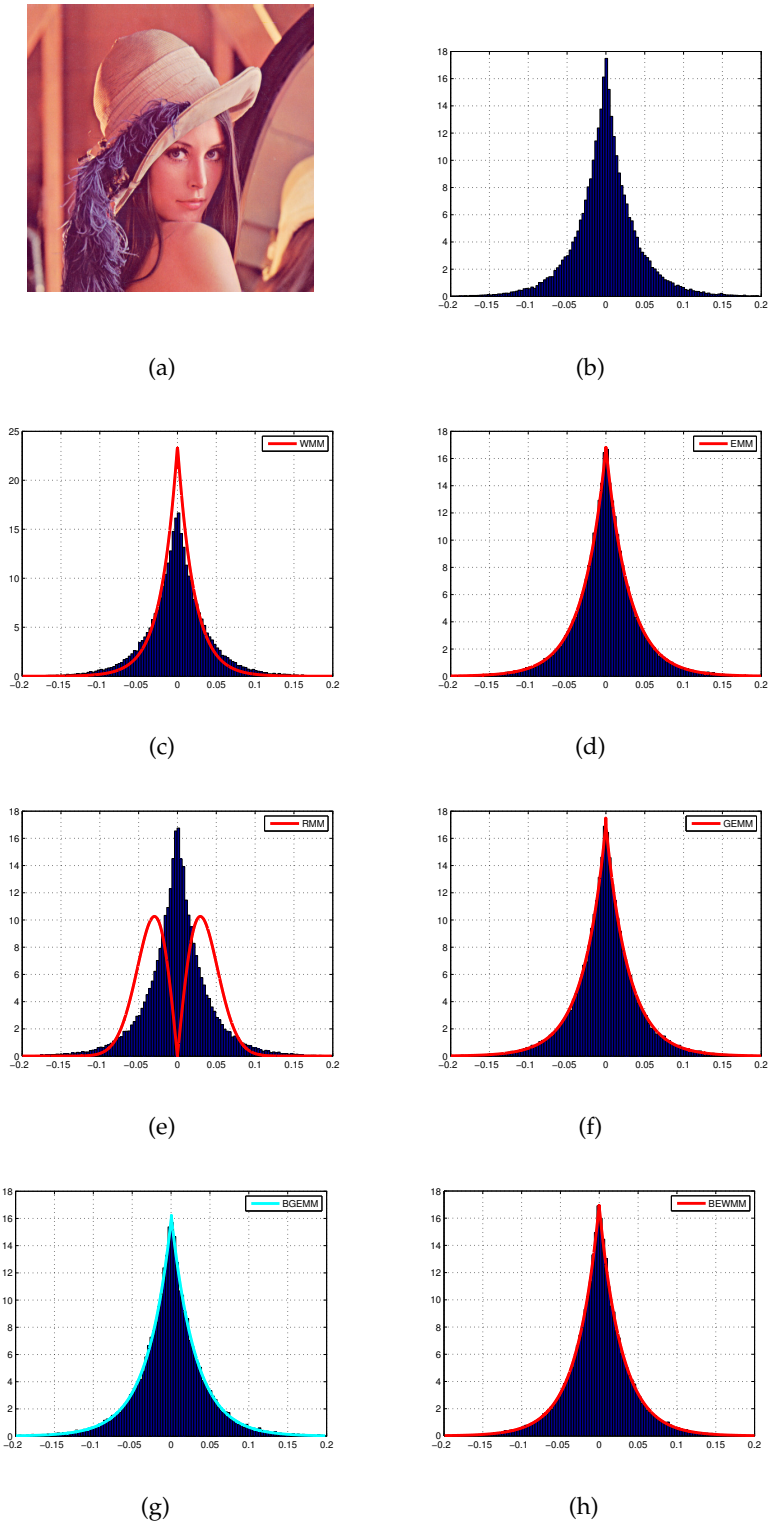

(a) (b) (c) (d) (e) (f) (g) (h)

FIGURE 5. Approximation of the wavelet coefficients with $K = 1$. (a) The original image (lena), (b) wavelet coefficients of high-pass subband (CH), (c) WMM ($\chi^2 = 3015.21$), (d) EMM ($\chi^2 = 16.03$), (e) RMM ($\chi^2 = 523.18$), (f) GEMM ($\chi^2 = 14.48$), (g) BGEMM ($\chi^2 = 13.81$), and (h) BEWMM ($\chi^2 = 13.69$).

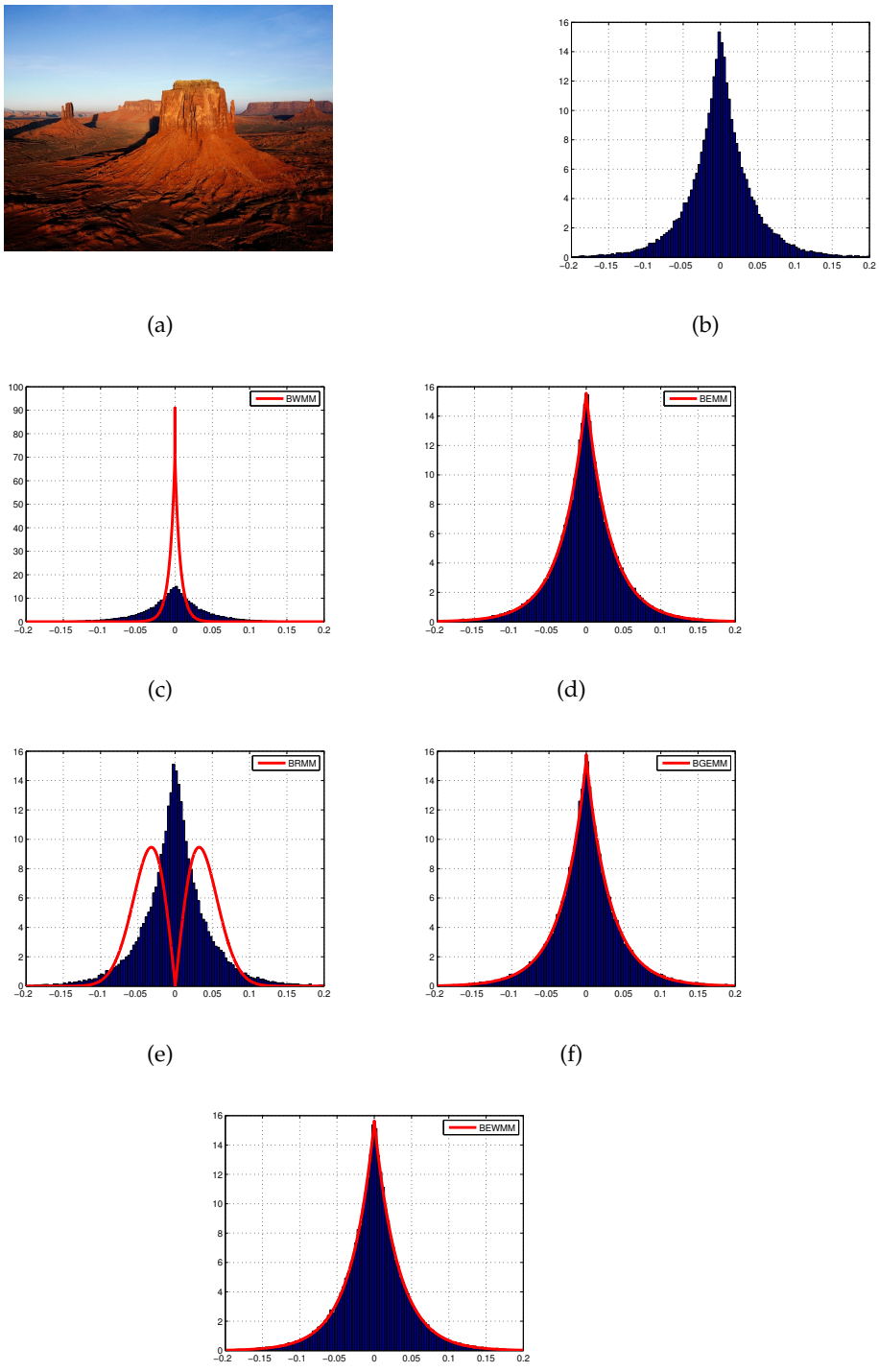

FIGURE 6. Approximation of the wavelet coefficients with $K = 1$. (a) The original image, (b) wavelet coefficients of high-pass subband (CH), (c) BWMM ($\chi^2 = 3300$), (d) BEMM ($\chi^2 = 15.07$), (e) BRMM ($\chi^2 = 621.33$), (f) BGEMM ($\chi^2 = 13.96$), and (g) BEWMM ($\chi^2 = 13.75$).

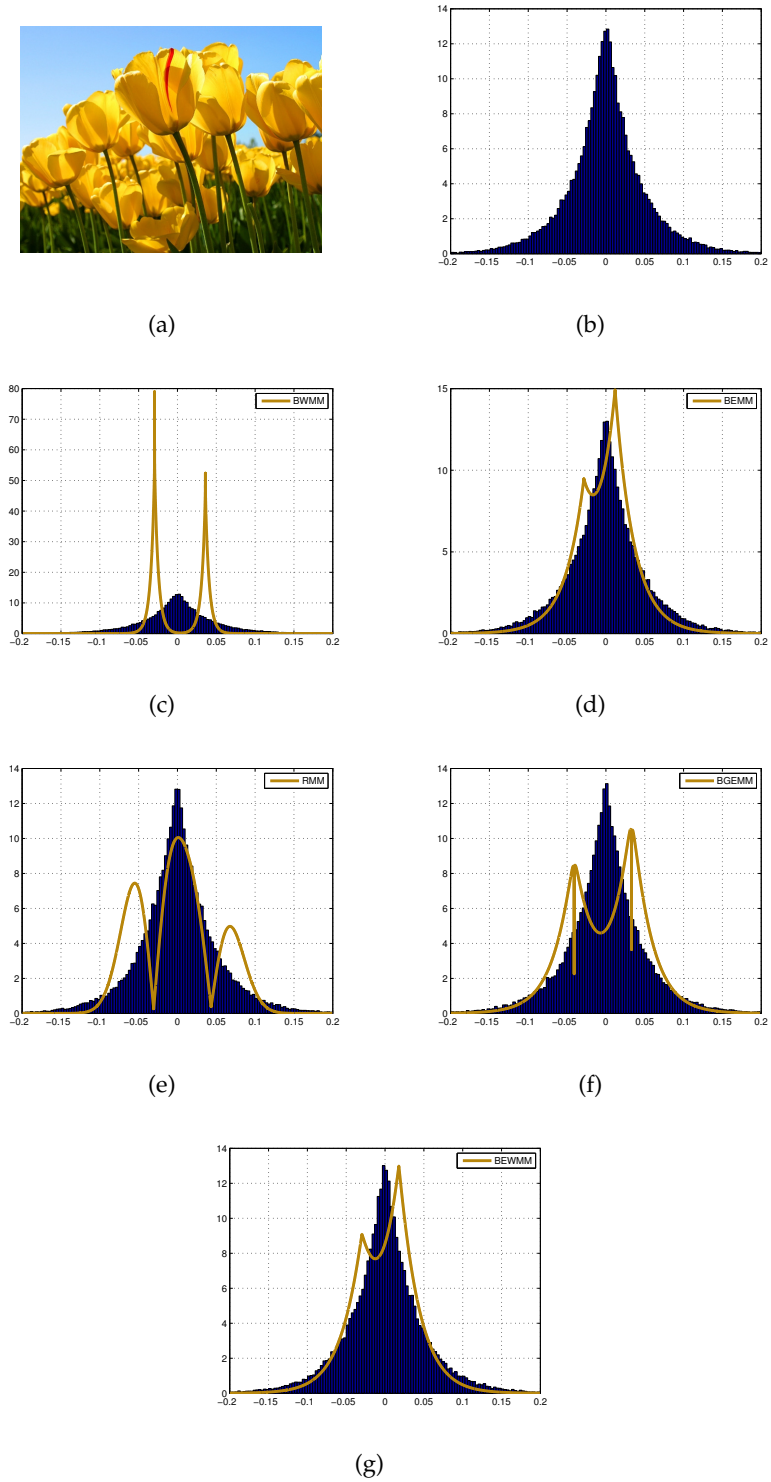

(a) (b) (c) (d) (e) (f) (g)

FIGURE 7. Approximation of the wavelet coefficients with $K = 2$. (a) The original image, (b) wavelet coefficients (level 3, CH), (c) BWMM ($\chi^2 = 1479.23$), (d) BEMM ($\chi^2 = 143.3$), (e) RMM ($\chi^2 = 230.09$), (f) BGEMM ($\chi^2 = 257$), and (g) BEWMM ($\chi^2 = 130.27$).

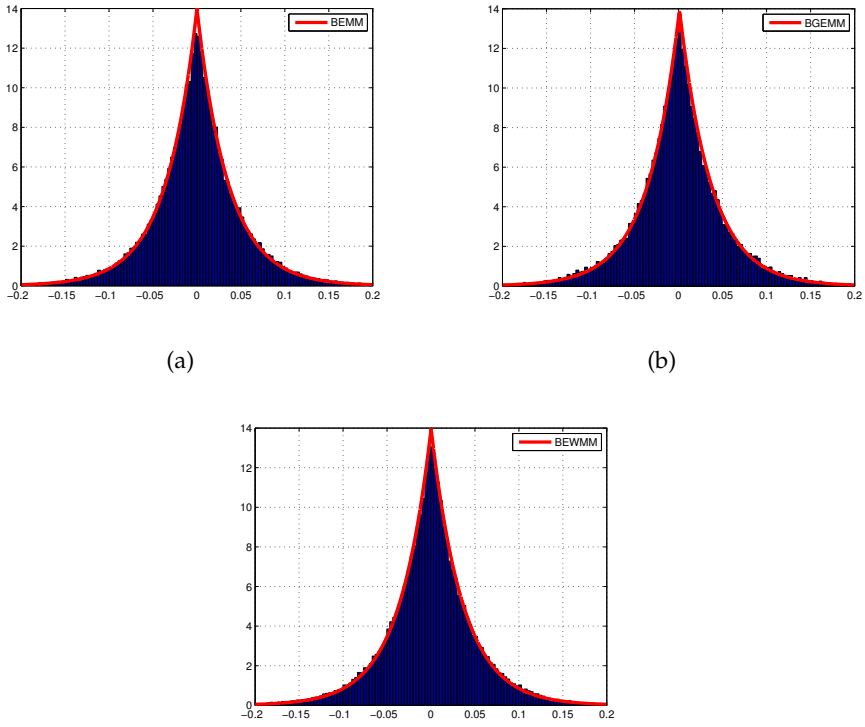

(a) (b)

(c)

FIGURE 8. Approximation of the wavelet coefficients (level 3, CH) with $K = 1$ for the previous image, (a) BEMM ($\chi^2 = 22.43$), (b) BGEMM ($\chi^2 = 20.33$), and (c) BEWMM ($\chi^2 = 19.89$).

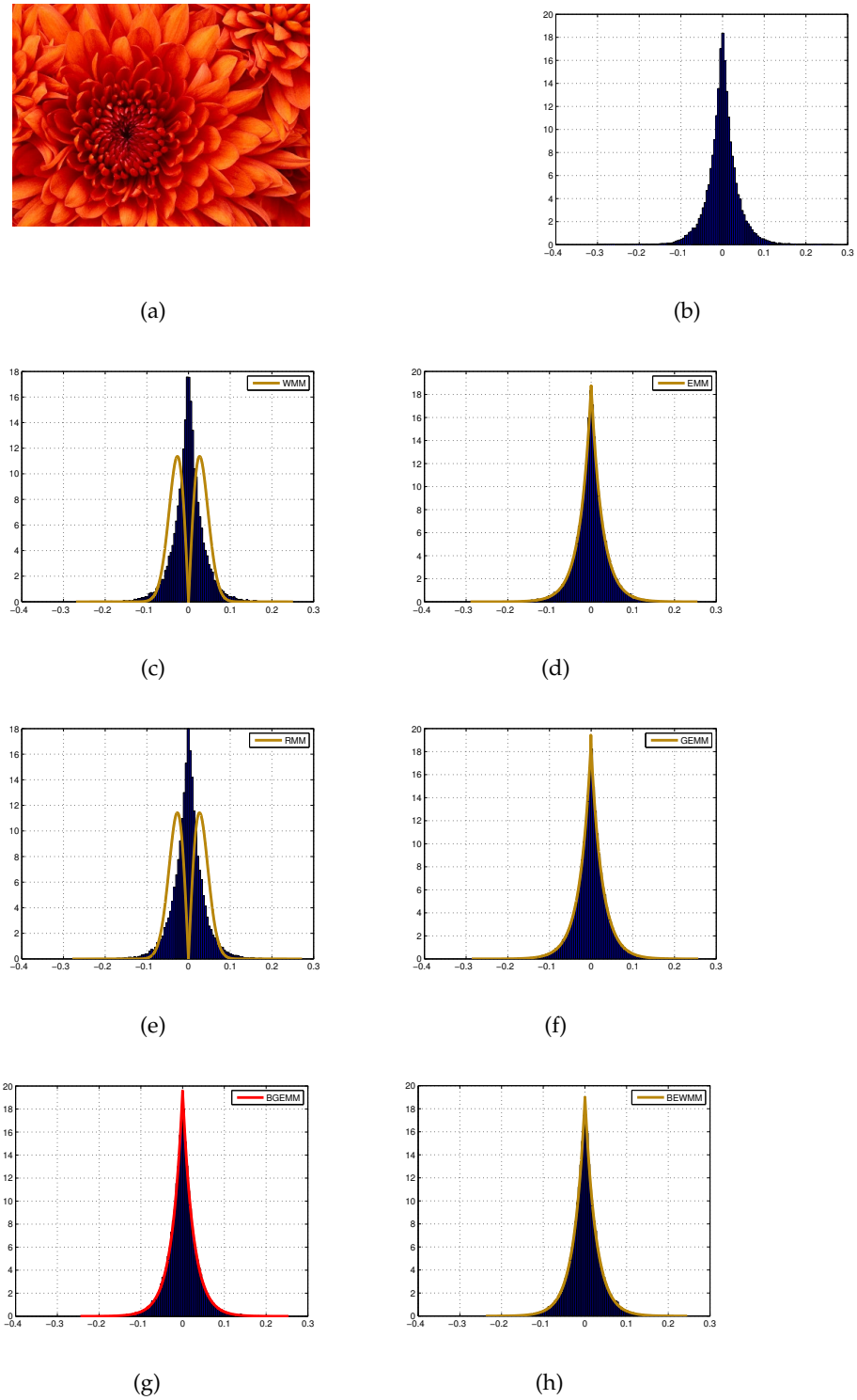

FIGURE 9. Approximation of the wavelet coefficients with $K = 1$. (a) The original image, (b) wavelet coefficients (level 2, CD), (c) WMM ($\chi^2 = 2150$), (d) EMM ($\chi^2 = 16$), (e) RMM ($\chi^2 = 2143.29$), (f) GEMM ($\chi^2 = 15.92$), (g) BGEMM ($\chi^2 = 15.87$), and (h) BEWMM ($\chi^2 = 15.73$).

Tables

TABLE 1. The comparative models are special cases of the BEWMM

EWMM	BEWMM: $\delta(x_i\|\Omega_j) = 1$, for all $j \in \{1,2,3,...,K\}$
BGEMM	BEWMM: $\gamma_j = 1$, for all $j \in \{1,2,3,...,K\}$
GEMM	BEWMM: $\delta(x_i\|\Omega_j) = 1$ and $\gamma_j = 1$, for all $j \in \{1,2,3,...,K\}$
BEMM	BEWMM: $\nu_j = 1$ and $\gamma_j = 1$, for all $j \in \{1,2,3,...,K\}$
EMM	BEWMM: $\delta(x_i\|\Omega_j) = 1$, $\nu_j = 1$ and $\gamma_j = 1$, for all $j \in \{1,2,3,...,K\}$
BWMM	BEWMM: $\nu_j = 1$, for all $j \in \{1,2,3,...,K\}$
WMM	BEWMM: $\delta(x_i\|\Omega_j) = 1$ and $\nu_j = 1$, for all $j \in \{1,2,3,...,K\}$
BRMM	BEWMM: $\nu_j = 1$ and $\gamma_j = 2$, for all $j \in \{1,2,3,...,K\}$
RMM	BEWMM: $\delta(x_i\|\Omega_j) = 1$, $\nu_j = 1$ and $\gamma_j = 2$, for all $j \in \{1,2,3,...,K\}$

TABLE 2. Log-likelihood (L), the corresponding AIC, CAIC and BIC values of models fitted to data in Figure 1.a

The model	-L	AIC	CAIC	BIC
WMM	281.13	578.26	578.2616	653.5205
GEMM	274.39	564.78	564.7816	640.0405
RMM	224.66	461.32	461.3209	517.7654
EWMM	200.96	421.92	421.9224	515.9956
BEWMM	200.07	420.14	420.1424	514.2156

TABLE 3. Log-likelihood (L), the corresponding AIC, CAIC and BIC values of models fitted to data in Figure 2.a

The model	-L	AIC	CAIC	BIC
WMM	230.57	467.14	467.1405	493.447
BWMM	230.11	466.22	466.2205	492.527
EMM	299.08	462.16	464.1605	479.698
BEMM	228.53	461.06	463.0603	478.598
GEMM	217.33	440.66	440.6605	466.967
BGEMM	216.58	439.16	439.1605	465.467
RMM	208.04	420.08	420.0803	437.618
BRMM	207.96	419.92	419.9203	437.458
EWMM	204.91	413.82	413.8203	431.358
BEWMM	204.07	412.14	412.1403	429.678

TABLE 4. Log-likelihood (L), the corresponding AIC, CAIC and BIC values of models fitted to data in Figure 3.a

The model	-L	AIC	CAIC	BIC
WMM	229.51	465.02	465.0205	491.327
BWMM	229.25	464.5	464.5005	490.807
BEMM	227.08	458.16	458.1603	475.698
GEMM	221.39	448.78	448.7805	475.087
BGEMM	220.14	446.28	446.2805	472.587
RMM	213.09	430.18	430.1803	447.718
EWMM	201.54	411.08	411.0808	446.156
BEWMM	201.32	410.64	410.6408	445.716

TABLE 5. Log-likelihood (L), the corresponding AIC, CAIC and BIC values of models fitted to data in Figure 4.a

The model	-L	AIC	CAIC	BIC
WMM	283.04	582.08	582.0816	657.3405
EMM	278.16	568.32	568.3209	624.7654
BEMM	227.51	567.02	567.0209	623.4659
GEMM	265.11	546.22	546.2216	621.4805
EWMM	252.88	525.76	525.7624	619.8356
BEWMM	252.67	525.34	525.3424	619.4156

TABLE 6. Log-likelihood (L), the corresponding AIC, CAIC and BIC values of models fitted to data in Figure 5.a

The model	-L	AIC	CAIC	BIC
WMM	229.37	464.74	464.7403	492.9627
RMM	226.5	457	457.0001	475.8151
EMM	219.33	442.66	442.6601	461.4751
GEMM	213.45	432.9	432.9003	461.1227
BGEMM	212.96	431.92	431.9203	460.1427
BEWMM	207.16	422.32	422.3204	459.9503

TABLE 7. Log-likelihood (L), the corresponding AIC, CAIC and BIC values of models fitted to data in Figure 6.a

The model	-L	AIC	CAIC	BIC
BWMM	234.08	474.16	474.1604	501.3575
BRMM	228.92	461.84	461.8402	479.9717
BEMM	227.26	458.52	458.5202	476.6517
BGEMM	220.13	446.26	446.2604	473.4575
BEWMM	212.87	433.74	433.7406	470.0033

TABLE 8. Log-likelihood (L), the corresponding AIC, CAIC and BIC values of models fitted to data in Figure 7.a, with $K = 2$

The model	-L	AIC	CAIC	BIC
BWMM	294.31	604.62	604.622	677.9741
BGEMM	283.56	583.12	583.122	656.4741
RMM	278.05	568.1	568.1012	623.1156
BEMM	276.91	565.82	565.8212	620.8356
BEWMM	253.78	527.56	527.5631	619.2527

TABLE 9. Log-likelihood (L), the corresponding AIC, CAIC and BIC values of models fitted to data in Figure 7.a, with $K = 1$

The model	-L	AIC	CAIC	BIC
BEMM	228.4	460.8	460.8002	479.1385
BGEMM	222.24	450.48	450.4803	478.7027
BEWMM	216.55	441.1	441.1006	477.7771

TABLE 10. Log-likelihood (L), the corresponding AIC, CAIC and BIC values of models fitted to data in Figure 9.a

The model	-L	AIC	CAIC	BIC
WMM	231.72	469.44	469.4404	496.6375
RMM	228.03	460.06	460.0602	478.1917
EMM	225.63	455.26	455.2602	473.3917
GEMM	219.29	444.58	444.5804	471.7775
BGEMM	218.73	443.46	443.4603	471.6827
BEWMM	213.4	434.8	434.8006	471.0633

Acknowledgements: The authors are extremely grateful to the reviewers for their valuable suggestions and leading a crucial role for a better presentation of this manuscript.

Authors' Contributions: All authors contributed equally to the writing of this paper. All authors read and approved the final manuscript.

Conflicts of Interest: The authors declare that there are no conflicts of interest regarding the publication of this paper.

References

[1] K. Copsey, A. Webb, Bayesian Gamma Mixture Model Approach to Radar Target Recognition, IEEE Trans. Aerosp. Electron. Syst. 39 (2003), 1201–1217. https://doi.org/10.1109/TAES.2003.1261122.

[2] A. Zellner, Bayesian and Non-Bayesian Analysis of the Log-Normal Distribution and Log-Normal Regression, J. Amer. Stat. Assoc. 66 (1971), 327–330. https://doi.org/10.1080/01621459.1971.10482263.

[3] Sylvia. Richardson, P.J. Green, On Bayesian Analysis of Mixtures with an Unknown Number of Components (with Discussion), J. R. Stat. Soc. Ser. B: Stat. Methodol. 59 (1997), 731–792. https://doi.org/10.1111/1467-9868.00095.

[4] J.M. Nicolas, F. Tupin, Gamma Mixture Modeled with "Second Kind Statistics": Application to SAR Image Processing, in: IEEE International Geoscience and Remote Sensing Symposium, IEEE, Toronto, Ont., Canada, 2002: pp. 2489–2491. https://doi.org/10.1109/IGARSS.2002.1026587.

[5] E.W. Stacy, A Generalization of the Gamma Distribution, Ann. Math. Stat. 33 (1962), 1187-1192. https://www.jstor.org/stable/2237889.

[6] G.S. Mudholkar, D.K. Srivastava, Exponentiated Weibull Family for Analyzing Bathtub Failure-Rate Data, IEEE Trans. Rel. 42 (1993), 299–302. https://doi.org/10.1109/24.229504.

[7] G.S. Mudholkar, D.K. Srivastava, M. Freimer, The Exponentiated Weibull Family: A Reanalysis of the Bus-Motor-Failure Data, Technometrics 37 (1995), 436–445. https://doi.org/10.1080/00401706.1995.10484376.

[8] G.S. Mudholkar, A.D. Hutson, The Exponentiated Weibull Family: Some Properties and a Flood Data Application, Commun. Stat. - Theory Methods 25 (1996), 3059–3083. https://doi.org/10.1080/03610929608831886.

[9] T. Eltoft, Modeling the Amplitude Statistics of Ultrasonic Images, IEEE Trans. Med. Imaging 25 (2006), 229–240. https://doi.org/10.1109/TMI.2005.862664.

[10] Kai-Sheng Song, Globally Convergent Algorithms for Estimating Generalized Gamma Distributions in Fast Signal and Image Processing, IEEE Trans. Image Process. 17 (2008), 1233–1250. https://doi.org/10.1109/TIP.2008.926148.

[11] M.N. Do, M. Vetterli, Wavelet-Based Texture Retrieval Using Generalized Gaussian Density and Kullback-Leibler Distance, IEEE Trans. Image Process. 11 (2002), 146–158. https://doi.org/10.1109/83.982822.

[12] S.K. Choy, C.S. Tong, Statistical Wavelet Subband Characterization Based on Generalized Gamma Density and Its Application in Texture Retrieval, IEEE Trans. Image Process. 19 (2010), 281–289. https://doi.org/10.1109/TIP.2009.2033400.

[13] M. Allili, Wavelet Modeling Using Finite Mixtures of Generalized Gaussian Distributions: Application to Texture Discrimination and Retrieval, IEEE Trans. Image Process. 21 (2012), 1452–1464. https://doi.org/10.1109/TIP.2011.2170701.

[14] J.W. Shin, J.H. Chang, S. Barbara, H.S. Yun, N.S. Kim, Voice Activity Detection Based on Generalized Gamma Distribution, in: IEEE International Conference on Acoustics, Speech, and Signal Processing, 2005., IEEE, Philadelphia, Pennsylvania, USA, 2005: pp. 781–784. https://doi.org/10.1109/ICASSP.2005.1415230.

[15] P. Kittisuwan, Image Denoising via Bayesian Estimation of Statistical Parameter Using Generalized Gamma Density Prior in Gaussian Noise Model, Fluct. Noise Lett. 14 (2015), 1550017. https://doi.org/10.1142/S0219477515500170.

[16] A.A. Farag, A.S. El-Baz, G. Gimel'farb, Precise Segmentation of Multimodal Images, IEEE Trans.Image Process. 15 (2006), 952–968. https://doi.org/10.1109/TIP.2005.863949.

[17] P. Hedelin, J. Skoglund, Vector Quantization Based on Gaussian Mixture Models, IEEE Trans. Speech Audio Process. 8 (2000), 385–401. https://doi.org/10.1109/89.848220.

[18] J. Lindblom, J. Samuelsson, Bounded Support Gaussian Mixture Modeling of Speech Spectra, IEEE Trans. Speech Audio Process. 11 (2003), 88–99. https://doi.org/10.1109/TSA.2002.805639.

[19] W. Weibull, A Statistical Distribution Function of Wide Applicability, J. Appl. Mech. 18 (1951), 293–297. https://doi.org/10.1115/1.4010337.

[20] D.N.P. Murthy, M. Xie, R. Jiang, Weibull Models, Wiley, 2003. https://doi.org/10.1002/047147326X.

[21] M. Bebbington, C.-D. Lai, R. Zitikis, A Flexible Weibull Extension, Reliab. Eng. Syst. Saf. 92 (2007), 719–726. https://doi.org/10.1016/j.ress.2006.03.004.

[22] T. Zhang, M. Xie, On the Upper Truncated Weibull Distribution and Its Reliability Implications, Reliab. Eng. Syst. Saf. 96 (2011), 194–200. https://doi.org/10.1016/j.ress.2010.09.004.

[23] A. Feldmann, W. Whitt, Fitting Mixtures of Exponentials to Long-Tail Distributions to Analyze Network Performance Models, Perform. Eval. 31 (1998), 245–279. https://doi.org/10.1016/S0166-5316(97)00003-5.

[24] G. McLachlan, D. Peel, Finite Mixture Models, Wiley, New York, 2000.

[25] L. Attardi, M. Guida, G. Pulcini, A Mixed-Weibull Regression Model for the Analysis of Automotive Warranty Data, Reliab. Eng. Syst. Saf. 87 (2005), 265–273. https://doi.org/10.1016/j.ress.2004.05.003.

[26] T. Bučar, M. Nagode, M. Fajdiga, Reliability Approximation Using Finite Weibull Mixture Distributions, Reliab. Eng. Syst. Saf. 84 (2004), 241–251. https://doi.org/10.1016/j.ress.2003.11.008.

[27] J.A. Carta, P. Ramírez, Analysis of Two-Component Mixture Weibull Statistics for Estimation of Wind Speed Distributions, Renew. Energy 32 (2007), 518–531. https://doi.org/10.1016/j.renene.2006.05.005.

[28] C. M. Bishop, Pattern Recognition and Machine Learning, Springer, Berlin, 2006.

[29] R.D. Gupta, D. Kundu, Generalized Exponential Distribution: Existing Results and Some Recent Developments, J. Stat. Plan. Inference 137 (2007), 3537–3547. https://doi.org/10.1016/j.jspi.2007.03.030.

[30] R.D. Gupta, D. Kundu, Theory & Methods: Generalized Exponential Distributions, Aust. N. Z. J. Stat. 41 (1999), 173–188. https://doi.org/10.1111/1467-842X.00072.

[31] K.V. Sorensen, S.V. Andersen, Rayleigh Mixture Model-Based Hidden Markov Modeling and Estimation of Noise in Noisy Speech Signals, IEEE Trans. Audio Speech Lang. Process. 15 (2007), 901–917. https://doi.org/10.1109/TASL.2006.885240.

[32] J. Seabra, F. Ciompi, P. Radeva, J.M. Sanches, A Rayleigh Mixture Model for IVUS Imaging, in: J.M. Sanches, A.F. Laine, J.S. Suri (Eds.), Ultrasound Imaging, Springer US, Boston, MA, 2012: pp. 25–47. https://doi.org/10.1007/978-1-4614-1180-2_2.

[33] P. Hedelin, J. Skoglund, Vector Quantization Based on Gaussian Mixture Models, IEEE Trans. Speech Audio Process. 8 (2000), 385–401. https://doi.org/10.1109/89.848220.

[34] J. Lindblom, J. Samuelsson, Bounded Support Gaussian Mixture Modeling of Speech Spectra, IEEE Trans. Speech Audio Process. 11 (2003), 88–99. https://doi.org/10.1109/TSA.2002.805639.

[35] T. Zhang, M. Xie, On the Upper Truncated Weibull Distribution and Its Reliability Implications, Reliab. Eng. Syst. Saf. 96 (2011), 194–200. https://doi.org/10.1016/j.ress.2010.09.004.

[36] M. Pereyra, N. Dobigeon, H. Batatia, J. Tourneret, Segmentation of Skin Lesions in 2-D and 3-D Ultrasound Images Using a Spatially Coherent Generalized Rayleigh Mixture Model, IEEE Trans. Med. Imaging 31 (2012), 1509–1520. https://doi.org/10.1109/TMI.2012.2190617.

[37] T.M. Nguyen, Q.M. Jonathan Wu, H. Zhang, Bounded Generalized Gaussian Mixture Model, Pattern Recognit. 47 (2014), 3132–3142. https://doi.org/10.1016/j.patcog.2014.03.030.

[38] P.J. Huber, Robust Statistics, Wiley, New York, 1981.

[39] J. Ashburner, K.J. Friston, Unified Segmentation, NeuroImage 26 (2005), 839–851. https://doi.org/10.1016/j.neuroimage.2005.02.018.

[40] H. Akaike, A New Look at the Statistical Model Identification, IEEE Trans. Autom. Control 19 (1974), 716–723. https://doi.org/10.1109/TAC.1974.1100705.

[41] P.J. Brockwell, R.A. Davis, Time Series: Theory and Methods, Springer, 1991.

[42] G. Schwarz, Estimating the Dimension of a Model, Ann. Stat. 6 (1978), 461-464.

[43] S.G. Chang, Bin Yu, M. Vetterli, Adaptive Wavelet Thresholding for Image Denoising and Compression, IEEE Trans. Image Process. 9 (2000), 1532–1546. https://doi.org/10.1109/83.862633.

[44] S. Kasaei, M. Deriche, B. Boashash, A Novel Fingerprint Image Compression Technique Using Wavelets Packets and Pyramid Lattice Vector Quantization, IEEE Trans. Image Process. 11 (2002), 1365–1378. https://doi.org/10.1109/TIP.2002.802534.